Violet photoluminescence from shell layer of Zn/ZnO core-shell nanoparticles induced by laser ablation

Haibo Zeng, Weiping Cai,[a] Jinlian Hu, Guotao Duan, Peisheng Liu, and Yue Li
Key Laboratory of Materials Physics, Anhui Key Laboratory of Nanomaterials and Nanotechnology, Institute of Solid State Physics, Chinese Academy of Sciences, Hefei 230031, People's Republic of China

(Received 12 December 2005; accepted 4 March 2006; published online 27 April 2006)

A strong violet photoluminescence (PL) band at 425 nm (2.92 eV) was observed from the ZnO shell layer of the Zn/ZnO core-shell nanoparticles prepared by laser ablation in liquid media. Such violet PL decreases with increase of the shell thickness or annealing temperature, showing good controllability. Based on the electron paramagnetic resonance measurements, the violet emission is attributed to the electronic transition from the defect level, corresponding to high-concentration zinc interstitials, to the valence band. This study is in favor to clarify the defect-related emissions and to extend the optical and electronic applications of nanostructured ZnO. © *2006 American Institute of Physics*. [DOI: 10.1063/1.2196051]

As a wide-band-gap semiconductor, wurtzite ZnO with a band-gap energy of 3.37 eV at room temperature and exciton binding energy of 60 meV is of many important applications in electronic and optical devices, especially in optoelectronic applications such as the ultraviolet (UV)/blue lasing media.[1] The optical properties of different structured (including nanostructured) ZnO have extensively been studied for several decades. In the photoluminescence (PL) spectra of ZnO, typically there are emission bands in the UV (Ref. 2) and visible (green,[3–7] blue,[8] and violet[9]) regions. The UV peak was usually considered as the characteristic emission of ZnO and attributed to the band edge emission or the exciton transition. Although the emissions in visible region were dominantly considered to be associated with the intrinsic defects in ZnO, there still exist extensive controversies in the dominant intrinsic defects.[10–14] Most researchers related the green emission to singly ionized oxygen vacancy based on the correlation between green PL and g value (=1.96) in electron paramagnetic resonance (EPR) measurements,[3–5] the aging effect,[6] and on the theoretical calculations of electronic structure, atomic geometry, and formation energy.[13,14] The blue[8] and violet[9] PL in ZnO are very unwonted and their mechanism studies are thus very limited. Wang *et al.* observed a violet PL at 402 nm from ZnO films deposited by rf magnetron sputtering and attributed it to the electronic transition from conduction band tail states to valence band tail states,[9] which is similar to the characteristic emission, and hence cannot represent the universal violet PL. Thereby, the in-depth understanding of the defect emission mechanism of the violet PL in ZnO still needs imperative investigation. Compared with the intensive studies about UV and green emissions in nanostructured ZnO, the investigation of violet emission has been very few due to its infrequency.

Previously, the Zn/ZnO core-shell structured nanoparticles were prepared by laser ablation of a zinc target in liquid media[15] at our laboratory. Recently, we have found a strong violet PL band at 425 nm (2.92 eV) from the ZnO shell layer in such composite nanoparticles, which is sensitive to the shell thickness and annealing conditions, but is much stronger than the characteristic (UV) and green emissions in the intensity. A g factor (2.05), different from that corresponding to the singly charged oxygen vacancy, was found. It has been indicated that the strong violet PL originates from the interstitial zinc defects formed during the laser-induced highly nonequilibrium microplasma process. The details are reported in this letter.

The laser ablation of a zinc target is performed in an aqueous solution with sodium dodecyl sulfate (SDS), as previously reported in details by our group[15] and others.[16–18] Briefly, a zinc plate (99.99%) was fixed on a bracket in a glass vessel filled with 10 ml SDS (99.5%) aqueous solution (0.05M). The plate was ablated for 30 min by the first harmonic of a Nd:YAG (yttrium aluminum garnet) laser (1064 nm, frequency of 10 Hz, and pulse duration of 10 ns) with the powers from 35 to 70 mJ/pluse. After ablation, all of the colloidal suspensions were centrifuged at 14 000 rpm, rinsed with ethanol for several times, and dried at room temperature. The structure of nanoparticles was investigated by x-ray diffraction (XRD) using Philips X'Pert with Cu $K\alpha$ line 0.154 19 nm, transmission electron microscopy (TEM, JEM-200CX), and highly resolved transmission electron microscopy (HRTEM, JEOL-2010). The room-temperature PL was measured using a HeCd laser excitation source (325 nm). The room-temperature EPR measurements were preformed using an EPR-200 spectrometer using an X band (about 9.65 GHz).

Figure 1(a) shows the typical XRD pattern for the sample obtained by laser ablation in 0.05M SDS aqueous solution with power of 70 mJ/pulse. Two sets of XRD peaks corresponding to metal Zn and wurtzite ZnO crystals were observed. TEM examination has revealed that the products consist of nearly spherical nanoparticles with average diameter about 20 nm, as shown in Fig. 1(b). HRTEM shows that the particles are of core-shell structure with zinc core and ZnO shell (the enlarged fringe image is not shown here). The thickness of ZnO shell decreases with the reduction of laser power, which is in agreement with a previous report.[15] The average thicknesses of ZnO shell are roughly 6, 3.8, and 2.5 nm corresponding to laser powers of 70, 50, and 35 mJ/pulse, respectively, in the 0.05M SDS solution, as typically shown in Figs. 1(c)–1(e).

[a]Author to whom correspondence should be addressed; electronic mail: wpcai@issp.ac.cn

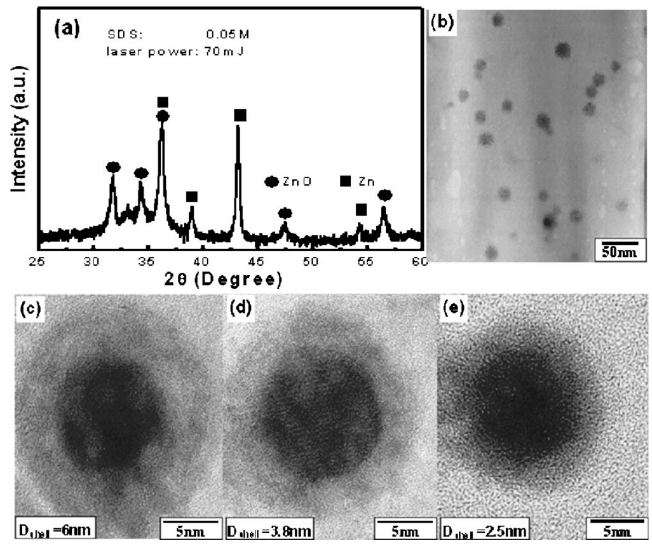

FIG. 1. XRD pattern (a) and TEM image (b) of Zn/ZnO nanoparticles obtained by laser ablation in 0.05*M* SDS aqueous solution with 70 mJ/pulse power. [(c)–(e)] HRTEM images for a single nanoparticles in the samples with different laser powers: 70, 50, and 35 mJ/pulse, respectively.

Figure 2 shows PL spectra of Zn/ZnO samples with different shell thicknesses. All samples exhibit a strong violet emission peak centered at 425 nm (2.92 eV) with an indistinct band tail in the green region, which is associated with oxygen vacancies in ZnO (Refs. 3–5) and is not discussed here. This violet emission and the tail increase with the decrease of shell thickness, but the peak position is almost unchanged. Such strong and near monochromatic violet PL has not been reported so far in nanostrucrured ZnO. Subsequent annealing will induce decrease of this emission, as illustrated in Fig. 3 corresponding to the sample with power of 70 mJ/pulse (the other samples show the similar results). The intensity of the violet emission decreases sharply with rise of annealing temperature up to 400 °C, at which the emission disappears completely and two other emission peaks are observed at UV (380 nm) and green (510 nm) bands, respectively. No trace of the consecutive shift of the violet emission is detected, indicating that such violet PL is a completely different emission from the conventional UV and green emissions. In addition, it is interesting that the primal

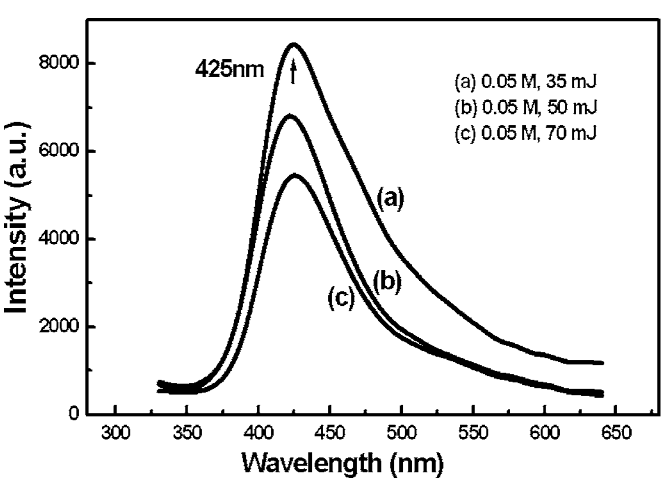

FIG. 2. PL spectra of Zn/ZnO nanoparticles obtained by laser ablation with different powers. (a) 35 mJ/pulse, (b) 50 mJ/pulse, and (c) 70 mJ/pulse.

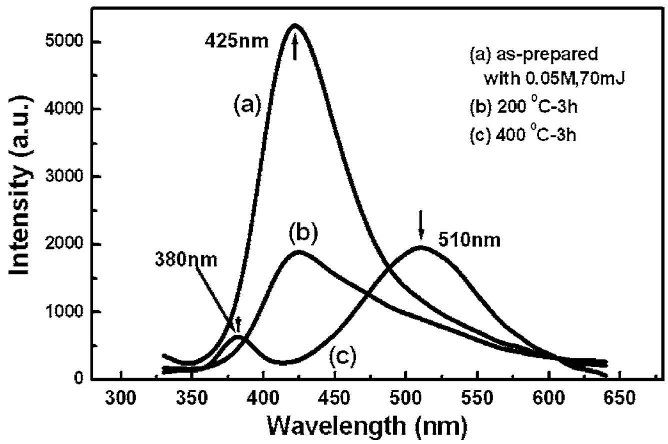

FIG. 3. PL spectra of Zn/ZnO nanoparticles obtained by laser ablation with 70 mJ/pulse before (a) and after annealing in atmosphere at 200 °C for 3 h (b) and 400 °C for 3 h (c), respectively.

violet PL is much stronger than the subsequent UV and green PL in this study.

The formation of core-shell structured Zn/ZnO nanoparticles has been demonstrated in a previous report[15] and will not be discussed here in details. Briefly, it can be attributed to the competition between aqueous oxidation and surfactant protection of Zn clusters, which are produced in the high-temperature and high-pressure zinc plasma on the solid-liquid interface quickly after the interaction between pulsed laser and the metal target. With decreasing laser power, the density and intensity of the hot plasma will be diminished greatly, leading to the reduction of the particle size (including the shell thickness).

As mentioned above, the shell thickness can be controlled from 6 to 2.5 nm, which is just in the range of the quantum size effect of nanostructured ZnO,[1–3] but no shift of the emission band with variance of the shell thickness was observed, demonstrating that the violet PL is not associated with the intrinsic emission of ZnO which induces the UV emission. From the annealing experiments, the violet PL is different from the UV and green emissions and should originate from a different kind of defects in ZnO from the familiar oxygen vacancies which induce the green emission.[3–5]

Lin *et al.*[7] have calculated the energy levels of various defect centers, such as vacancies of oxygen and zinc, interstitial oxygen and zinc, and antisite oxygen in ZnO. The energy gap between the conduction band and the level of oxygen vacancies is considered to be 2.28 eV and that from the interstitial zinc level to the valence band is 2.9 eV. The latter is very well consistent with the energy of the violet PL in this study. Moreover, according to some defect centers given by Kroger[19] and Bylander,[20] the defect energy level of interstitial zinc is considered to be 0.22 eV below the conduction band edge when the band gap of ZnO is 3.2 eV, which is also in agreement with our results. Hereby, we attribute the violet PL from the ZnO shell layer in the Zn/ZnO nanoparticles to the radiative transition of electrons from the local defect level of interstitial zinc to the valence band.

It is reasonable that there exists interstitial zinc in ZnO lattices, even as the dominant intrinsic defect, since the nanoparticles are very quickly formed in the extreme conditions[21–23] or the high-temperature and high-pressure zinc plasma, and the subsequent rapid reactive quenching, induced by laser ablation in the liquid media. Previous the-

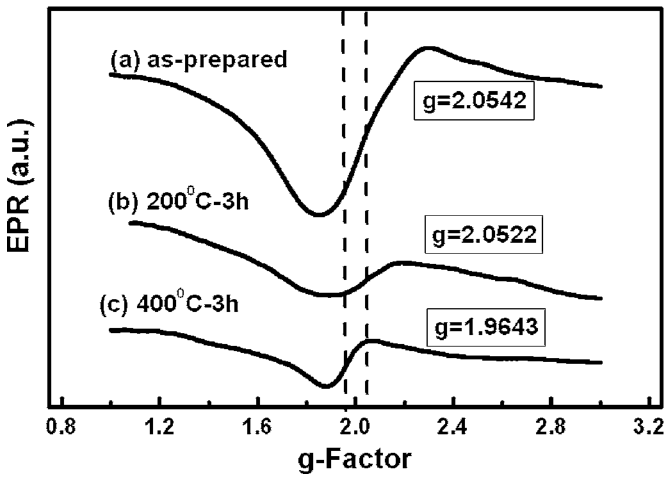

FIG. 4. EPR spectra of Zn/ZnO nanoparticles obtained by laser ablation with 70 mJ/pulse before (a) and after annealing in atmosphere at 200 °C for 3 h (b) and 400 °C for 3 h (c), respectively.

oretical investigations indicated that the formation energy of oxygen vacancy is much lower than that of interstitial zinc in the equilibrium defect formation process,[12–14] which should be the reason why the violet PL and interstitial zinc defect are very unwonted in usual nanostructured ZnO. However, in the laser-induced extreme conditions, the high-concentration zinc interstitial defect could be quickly and availably "frozen" (remained) in the ZnO shell layer.

For further confirmation, the EPR measurements were implemented. The results were shown in Fig. 4. For the sample (annealed in 400 °C) with green emission, the value of g factor $g=1.9652$ was obtained, which is well in coincidence with the previous report and related to the singly ionized oxygen vacancies.[3–5] For the samples (as prepared and annealed in 200 °C) with violet emission, however, the g factor is about 2.05. More importantly, there exists good positive correlation between the evolution of intensity of the violet PL and the signal of 2.05 g factor with annealing. Such violet-PL-correlated g factor confirms that the violet PL should originate from other kind of defects than oxygen vacancies. Obviously, the effect of impurities and surface states can be excluded due to the intensity of the signal. From the electron configuration, we know that there are four possible paramagnetic defects: singly charged oxygen and zinc vacancies and interstitial oxygen and zinc in ZnO. In our case, the laser-induced high-temperature and high-pressure zinc plasma would induce the fast formation of ZnO shell during subsequent fast extinguishment of the plasma.[15] Such nonequilibrium process would very easily lead to high concentration of Zn interstitials in ZnO and oxygen deficiency. The analyses above demonstrate that the results of violet emission and 2.05 g factor are all associated with the zinc interstitials in ZnO. It is due to the extreme conditions induced by laser that we can obtain such nanoparticles with the special structure and hence unique properties.

In addition, with decrease of the applied laser power, the plasma plume will become weaker and its lasting time will become shorter. This would lead to the faster formation of ZnO shell layer, accompanied by the reduction of shell thickness[15] and hence increase of concentrations of Zn interstitials and oxygen vacancies, inducing the enhancement of violet emission and its tail in the green region (see Fig. 2).

In summary, we observed the strong violet PL at 425 nm from the ZnO shell of core-shell Zn/ZnO nanoparticles prepared by laser ablation in liquid media. Such violet PL can be well controlled by adjusting the ZnO shell thickness or annealing. The emission energy of the violet PL agrees well with the reported energy level of interstitial zinc. Such violet emission likely originates from the radiative transition of electrons from the local interstitial zinc level to the valence band. It is just due to the extreme conditions induced by laser process that the unique nanostructures can be formed and hence the strong violet PL is observed. The strong violet PL and corresponding high-concentration Zn interstitial defect are expected to further clarify the mechanisms of defect emission and extend the optical and electronic applications of nanostructured ZnO.

This project is financially supported by the National Natural Science Foundation of China (Grant Nos. 50271069 and 10474099) and National Project for Basic Research Grant No. 2006CB300402.

[1]M. H. Huang, S. Mao, H. Feick, H. Yan, Y. Wu, H. Kind, E. Weber, R. Russo, and P. Yang, Science **292**, 1897 (2001).
[2]E. M. Wong and P. C. Searson, Appl. Phys. Lett. **74**, 2939 (1999).
[3]K. Vaheusden, C. H. Seager, W. L. Warren, D. R. Tallant, and J. A. Voigt, Appl. Phys. Lett. **68**, 403 (1996).
[4]K. Vanheusden, W. L. Warren, C. H. Seager, D. R. Tallant, J. A. Voigt, and B. E. Gnada, J. Appl. Phys. **79**, 7983 (1996).
[5]C. M. Mo, Y. H. Li, Y. S. Liu, Y. Zhang, and L. D. Zhang, J. Appl. Phys. **83**, 4389 (1998).
[6]F. K. Shan, G. X. Liu, W. J. Lee, G. H. Lee, I. S. Kim, and B. C. Shin, Appl. Phys. Lett. **86**, 221910 (2005).
[7]B. X. Lin, Z. X. Fu, and Y. B. Jia, Appl. Phys. Lett. **79**, 943 (2001).
[8]J. J. Wu and S. C. Liu, Adv. Mater. (Weinheim, Ger.) **14**, 215 (2002).
[9]Q. P. Wang, D. H. Zhang, Z. Y. Xue, and X. T. Hao, Appl. Surf. Sci. **201**, 123 (2002).
[10]K. I. Hagemark, J. Solid State Chem. **16**, 293 (1976).
[11]G. D. Mahan, J. Appl. Phys. **54**, 3825 (1983).
[12]F. Oba, S. R. Nishitani, S. Isotani, H. Adachi, and I. Tanaka, J. Appl. Phys. **90**, 824 (2001).
[13]A. F. Kohan, G. Ceder, D. Morgan, and C. G. Van de Walle, Phys. Rev. B **61**, 15019 (2000).
[14]S. B. Zhang, S. H. Wei, and A. Zunger, Phys. Rev. B **63**, 075205 (2001).
[15]H. B. Zeng, W. P. Cai, Y. Li, J. L. Hu, and P. S. Liu, J. Phys. Chem. B **109**, 18260 (2005).
[16]F. Mafune, J. Y. Kohno, Y. Takeda, T. Kondow, and H. Sawabe, J. Phys. Chem. B **105**, 5114 (2001).
[17]C. C. Huang, C. S. Yeh, and C. J. Ho, J. Phys. Chem. B **108**, 4940 (2004).
[18]H. Usui, Y. Shimizu, T. Sasaki, and N. Koshizaki, J. Phys. Chem. B **109**, 120 (2005).
[19]F. A. Kroger, *The Chemistry of Imperfect Crystals* (North-Holland, Amsterdam, 1964), p. 691.
[20]E. G. Bylander, J. Appl. Phys. **49**, 1188 (1978).
[21]P. P. Patil, D. M. Phase, S. A. Kulkarni, S. V. Ghaisas, S. K. Kulkarni, S. M. Kanetkar, S. B. Ogale, and V. G. Bhide, Phys. Rev. Lett. **58**, 238 (1987).
[22]S. B. Ogale, P. P. Patil, D. M. Phase, Y. V. Bhandarkar, S. K. Kulkarni, S. Kulkarni, V. G. Bhide, and S. Guha, Phys. Rev. B **36**, 8237 (1987).
[23]K. Saito, T. Sakka, and Y. Ogata, J. Appl. Phys. **94**, 5530 (2003).